INTERNATIONAL JOURNAL OF CLIMATOLOGY
*Int. J. Climatol.* **25**: 997–1006 (2005)
Published online in Wiley InterScience (www.interscience.wiley.com). DOI: 10.1002/joc.1177

# AN OVERVIEW OF THE AIRFLOW DISTORTION AT ANEMOMETER SITES ON SHIPS

BENGAMIN I. MOAT,[a,*] MARGARET J. YELLAND,[a] ROBIN W. PASCAL[a] and ANTHONY F. MOLLAND[b]
[a] *National Oceanography Centre, Southampton, UK*
[b] *School of Engineering Sciences, Ship Science, University of Southampton, Southampton, UK*

*Received 2 May 2004*
*Revised 6 September 2004*
*Accepted 11 October 2004*

## ABSTRACT

Wind speed measurements obtained from ship-mounted anemometers are biased by the presence of the ship itself distorting the flow of air to the anemometer. Recent studies have used numerical models to simulate the flow around very detailed representations of individual research ships in order to quantify the effects of flow distortion at the anemometer locations. Such anemometers are generally in well-exposed positions, typically on a mast in the bows of the ship. In contrast, very little is known about the possible effects of airflow distortion on the wind speed measurements from fixed anemometers on Voluntary Observing Ships (VOS). This is because (1) the several thousand or so merchant vessels vary significantly in shape and size and it would be impractical to study each individual ship, and (2) the anemometer location is not usually known.

This paper describes initial results from a study of flow distortion over 'typical' tankers and bulk carriers. A method to describe the shapes of these VOS and container ships is presented. The influence of distortion on the flow above the bridges of VOS is shown to be significant, with possible biases in the measured wind speed of between +11% and −100%, depending on the anemometer location. Recommendations for the siting of anemometers are made. 

KEY WORDS: wind speed error; VOS; ICOADS; CFD

## 1. INTRODUCTION

Research ships are traditionally used to gather high-quality marine meteorological data, but their coverage of the world's oceans is very limited. In contrast, merchant ships continuously travel across the world's oceans and cover more of the oceans than a single research ship can in its lifetime. As a consequence, a large proportion of the merchant fleet is recruited to the World Meteorological Organization's (WMO) Voluntary Observing Ships (VOS) programme to report meteorological parameters at the ocean surface routinely. Over many years these meteorological observations have been collated in the International Comprehensive Ocean–Atmosphere Data Set (ICOADS; Diaz *et al*., 2002). ICOADS is used for ocean–atmosphere model forcing, coupled ocean–atmosphere model validation, satellite validation and to create gridded data sets and climatologies to quantify and predict possible changes in climate.

Some of the wind speed reports from VOS are derived from visual observations of sea state, whereas others are obtained from anemometers mounted on the ship. It has long been suspected that wind speed measurements from anemometers may be affected by the presence of the ship distorting the flow of air (Dobson, 1981), resulting in measured wind speeds that are accelerated or decelerated compared with the free stream, or undisturbed, flow. Until recently, neither the magnitude nor the sign of such biases was known.

* Correspondence to: Bengamin I. Moat, James Rennell Division for Ocean Circulation and Climate, National Oceanography Centre, European Way, Southampton, SO14 3ZH, UK; e-mail: bim@noc.soton.ac.uk

Section 2 of this paper summarizes recent studies that have addressed the problem of flow distortion at specific anemometer locations on individual research ships. These studies used detailed models of individual ships, an approach which is not suited to the sheer numbers of ships incorporated in the VOS fleet. Section 3 describes the approach taken in the current study, whereby generic or typical VOS ship shapes are determined in order to represent three types of VOS (tankers, bulk carriers and container ships). Initial results of numerical models over these generic VOS are then described. Section 4 discusses possible implications of these results.

## 2. RESEARCH SHIPS

Previous work to determine the wind speed bias due to the airflow distortion caused by airflow around ships' structures has mainly been concerned with oceanographic research ships. One qualitative approach compared wind speed measurements from anemometers on masts with those from anemometers on booms projecting from a ship's bow (Ching, 1976; Kidwell and Seguin, 1978). When the ships were beam on to the wind, Ching (1976) found that the mast wind speed measurements were biased high compared with those made from anemometers on the bow booms. The minimum difference between measurements occurred when the wind was directly over the bow. Kidwell and Seguin (1978) showed similar results, and stated that the differences in wind speeds measured using mast and boom sensors depended upon the relative wind direction, the wind speed, the sensor height above sea level and the exposure of the sensor to the wind.

A number of wind-tunnel studies of ships have been made. Mollo-Cristensen (1979) used a wind-tunnel study of the R/V *Flip* to demonstrate that bow-mounted anemometers have to be located at a distance greater than the windward cross-section of the vessel to achieve a wind speed measurement accurate to within $\pm 5\%$. Wind-tunnel tests were carried out by Romanov *et al*. (1983) for the Russian R/V *Akademik Mstislav Keldysh*, by Surry *et al*. (1989) and Thiebaux (1990) for three Canadian research ships and by Blanc (1986, 1987) for two naval ships. Underestimates of the wind speed of 5% at the end of a bow boom and 3% for the foremast anemometer site were measured for the R/V *Akademik Mstislav Keldysh* for airflow over the bows, whereas the Canadian research ships showed overestimates of the wind speed of 5 to 10% for the main mast anemometer sites for most relative wind directions.

As computing power increases, numerical modelling of the airflow around ships has become an attractive alternative to the use of wind tunnels. Computational fluid dynamics (CFD) models allow wind speed errors to be determined from any number of anemometer locations, for a variety of wind speeds and wind directions. CFD studies have varied in complexity from computationally inexpensive potential flow models to large-eddy simulation (LES) models. Kahma and Leppäranta (1981) solved the flow field around a two-dimensional ship profile of the *RV Aranda* using simple potential flow theory. Potential flow models simulate the flow of an ideal fluid but are of limited use as they do not reproduce some crucial features of a real flow, e.g. flow separation. Nevertheless, their study gave the first insight into the magnitude of the flow distortion at anemometer sites on ships. Dupius (personal communication, 1994) used a simple two-dimensional CFD model to predict a wind speed increase of about 20% at the main mast anemometer site on R/V *Le Suroit*. Such two-dimensional models may overestimate the effects of flow distortion since, in reality, the flow is deflected in the horizontal as well as the vertical. More recently, three-dimensional CFD simulations have been used to calculate both the wind speed bias and the displacement of the flow to the anemometer site. Yelland *et al*. (1998, 2002) used three-dimensional CFD models to predict the airflow distortion at particular anemometer sites on 11 research ships. Dupius *et al*. (2003) studied the three-dimensional airflow over the R/V *L'Atalante*. Popinet *et al*. (2004) used the LES code GERRIS (freely available at http://gfs.sourceforge.net/) to study the unsteady flow around the R/V *Tangaroa*. All these studies showed that the wind speed bias is strongly dependent on the angle of the ship to the wind, but largely independent of the wind speed.

Yelland *et al*. (2002) showed that the likely wind speed biases for anemometers located on ships' main masts above the superstructure are of the order of 5%, and that anemometers on masts in the ships' bows may experience flows that have been decelerated by between 0 and 15%.

In all the above studies the ship geometries were very detailed and the anemometers were carefully sited in well-exposed locations, such as a foremast in the ship's bow. In contrast, anemometers on VOS are generally

 

located above the bridge, where the flow distortion may be more severe. Performing detailed models of the large number of VOS is not practical.

## 3. AIRFLOW OVER TYPICAL VOS

### *3.1. Introduction*

Until recently there have been few studies of the airflow over VOS. A combination of CFD simulations and wind-tunnel testing of the wind loads on a ferry was undertaken by Aage *et al*. (1997) to determine the ship's manoeuvrability in a harbour. Jin *et al*. (2001) used a CFD model of the flow over a merchant ship to observe the influences of the funnel and accommodation arrangement on the smoke behaviour. Neither study was aimed at quantifying possible biases in VOS wind speed measurements.

The VOS fleet contains several thousand merchant ships of various types, sizes and shapes. Of these, about 10% leave the VOS fleet and are replaced by other ships each year (E. Kent, personal communication, 2002). It is clearly not feasible to model the flow of air around each individual VOS. However, the fleet may be split into various types of ship and a generic, or typical, ship shape (Section 3.2) can be used to represent each type. The distribution by ship type of the world fleet (ISL, 1997), the VOS fleet and the subset of VOS included in the VOSClim project (JCOMM, 2002) are shown in Figure 1. VOSClim aims to provide a high quality set of marine meteorological observations with accompanying metadata on the ship, instruments and observing methods. The distributions differ, since the VOSClim ships are all open-ocean vessels, whereas the world and VOS fleets include many small coastal vessels. Taken together, the tankers, bulk carriers and container ships represent 53% of the VOSClim fleet, 39% of the world fleet and 40% of the VOS fleet. The largest proportion of ships within the world and VOS fleets are general cargo ships.

### *3.2. Generic ship models*

This section summarizes the method used by Moat (2003) to define simple bluff body, or 'block-like', representations of tankers, bulk carriers and container ships. Unfortunately, no ship dimensions were available to create a representation of a general cargo ship. Moat (2003) showed that the shapes of tankers and bulk carriers are very similar and can be treated together as one type. Ship dimensions were obtained for a total of 44 tanker and bulk carriers (RINA Ltd, 1990–93). Linear regressions were fitted to the various dimensions against the ship length overall (LOA). The coefficients for each regression are listed in Table I. The resulting equations were used to create a generic bluff body representation of a tanker/bulk carrier. This is shown in Figure 2.

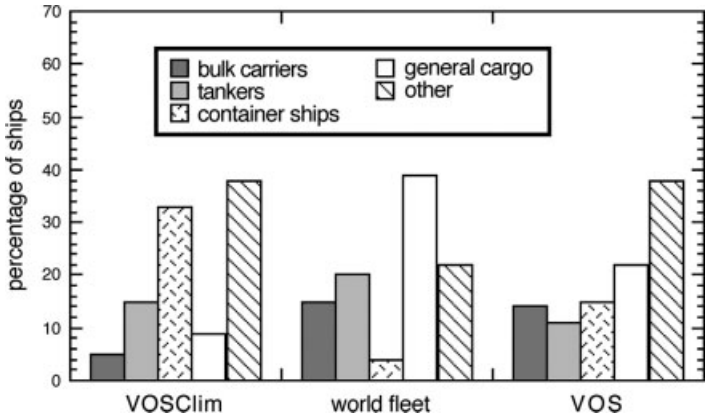


Figure 1. Merchant ships as a proportion of the VOSClim project (JCOMM, 2002), as a percentage of the world fleet (ISL, 1997) and VOS fleet in 1999

 

Table I. Coefficients of a linear fit model to describe the shape of a generic tanker and bulk carrier of any length (LOA). The principal dimensions are illustrated in Figure 2

| Ship dimension ($= a + b \times \mathrm{LOA}$) | $a$ | $b$ |
|---|---|---|
| Bridge to waterline BH | 10.65 | 0.0515 |
| Freeboard $F$ | 1.54 | 0.0254 |
| Bridge length $L$ | 10.16 | 0.0198 |
| Breadth $B$ | −3.00 | 0.1800 |
| Bridge to deck $H$ $(H = \mathrm{BH} - F)$ | 9.11 | 0.0260 |

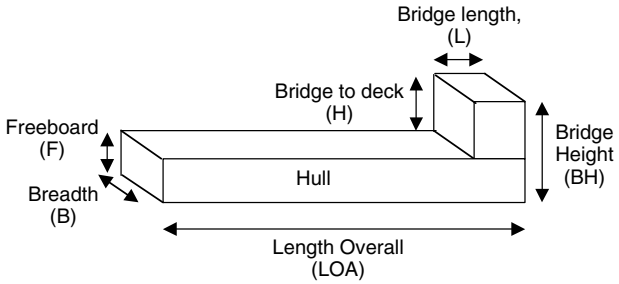


Figure 2. The shape and principal dimensions of a block geometry representation of a tanker/bulk carrier. Note: not to scale

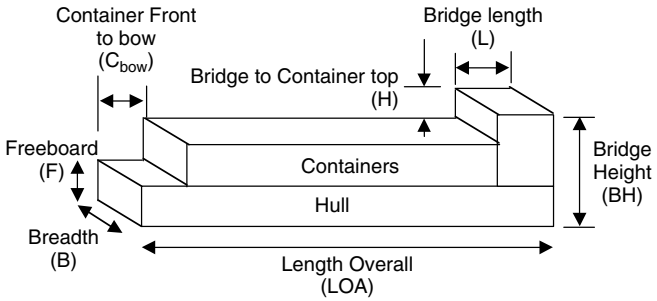


Figure 3. Illustration showing the dimensions of a forward-loading generic representation of a container ship. Note: not to scale

Similar dimensions were also obtained for 27 container ships (RINA Ltd, 1990–93). Container ships are of two main designs: first, ships with containers loaded in front of the bridge (Figure 3) and, second, larger ships with containers loaded in front of and behind the deck house (Figure 4). Linear regressions were fitted to the dimensions of both ship designs against the ship LOA (Table II) and used to generate a generic model of each.

The generic ship shapes clearly differ in many ways from a real ship structure. For example: the bow is a broad flat shape rather than a curved surface; the deckhouse spans the whole breadth of the ship; and masts, satellite communication domes and other small-scale obstructions are not included in the model. For these reasons the results of the numerical simulations of the flow over generic merchant vessels (Section 3.3) will represent the flow distortion caused by the large-scale obstruction of the ships hull and superstructure only. The generic models are applicable to tankers and bulk carriers that do not have deck-mounted cargo-handling equipment. It is noted that some bulk carriers do have large deck cranes, which would promote turbulence upstream of the bridge and could modify the airflow over the bridge. It is the absence of small-scale obstructions that is thought to be the most significant difference between the generic and the real ship

 

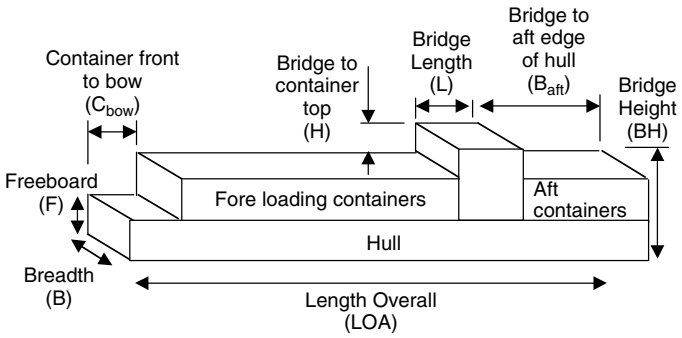


Figure 4. Illustration showing the dimensions of a fore-and-aft loading generic representation of a container ship. Note: not to scale

Table II. Coefficients of the linear fit model to describe two types of generic container ship of any length (LOA). The principal dimensions are illustrated in Figures 3 and 4

| Ship dimension ($= a + b \times$ LOA) | Forward loading | | Forward and aft loading | |
|---|---|---|---|---|
| | *a* | *b* | *a* | *b* |
| Bridge top to waterline BH | 5.54 | 0.1200 | 10.95 | 0.0770 |
| Freeboard *F* | 0.66 | 0.0559 | 5.37 | 0.0290 |
| Bridge length *L* | −0.91 | 0.0768 | 2.96 | 0.0442 |
| Breadth *B* | 2.28 | 0.1450 | 15.32 | 0.0670 |
| Bridge to container top *H* | −0.03 | 0.0301 | 1.20 | 0.0230 |
| Bow to container front $C_{bow}$ | 4.63 | 0.0755 | 18.70 | 0.0028 |
| Bridge aft to aft edge of hull $B_{aft}$ | Not used | Not used | −13.16 | 0.2540 |

shape. In reality, an instrument mounted on a mast would also be affected by the flow distortion caused by the mast itself. The extent of this distortion depends primarily on the distance between the mast and the instrument (Gill *et al*., 1967). However, such information is not presently available, even in the VOSClim metadata.

### *3.3. Numerical modelling of generic VOS*

The commercially available CFD code VECTIS was used to model the flow over the three-dimensional generic VOS shapes described in Section 3.2. Details of the code and the methodology are given by Moat (2003) and will only be described briefly here. VECTIS was used to calculate the three-dimensional, compressible, steady-state solutions of the Navier–Stokes continuity and energy equations. The code has previously been used to study the airflow over many research ships (Yelland *et al*., 2002). The main advantage of VECTIS over other CFD codes used to study airflow over ships is its ability to create computational meshes quickly and efficiently. In addition, Dupius *et al*. (2003) found that they were not able to predict the vertical displacement of the airflow to the anemometer locations using another commercial CFD code. Generally, the simulations took up to 3 to 4 weeks to converge using an Origin 200 UNIX workstation. Only airflows directly over the bow (head to wind) were considered in detail, but preliminary results for wind directions up to 30° from the bow show little variation in the pattern of the flow. Since merchant ships generally travel at speeds of 5 to 10 m $s^{-1}$, the apparent wind direction is predominantly over the bow. For example, a 1 month sample of COADS data (November 1986) showed that over 40% of the merchant ships' observations were obtained for relative wind directions within ±25° of the bow.

Figure 5 shows the flow pattern above the tanker/bulk carrier model. A standing vortex is produced in front of the bridge and there is flow separation at the upwind edge of the bridge. Close to the top of the bridge the airflow is decelerated and a weak flow counter to the mean flow direction is present. The depth of

 

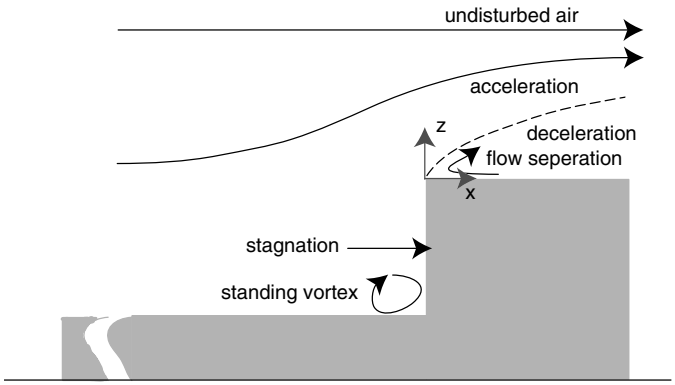


Figure 5. The general flow pattern above the bridge of a generic tanker/bulk carrier. The dashed line indicates the 'line of equality', where the wind speed is equal to the free stream wind speed. The mean flow is from left to right and the origin of the coordinate system is displayed

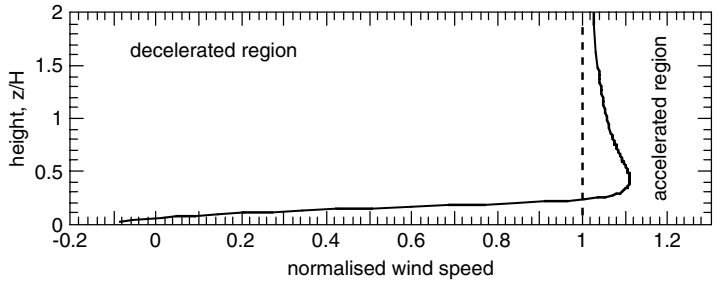


Figure 6. Normalized wind speed profile above the tanker/bulk carrier at a distance of $x/H = 0.5$ back from the front edge of the bridge ($x/H = 0 = z/H$). The wind speed profile has been normalized by the free stream, or undisturbed, wind speed profile. Adapted from Moat *et al.* (2004)

the decelerated region increases with distance back from the front edge of the bridge. Above the decelerated region is a line of equality where the wind speed is equal to the free stream wind speed. Directly above and below the line of equality the velocity gradients are very steep, making the wind speed bias very sensitive to the exact location of the anemometer. Above the line of equality the wind speed is accelerated and then decreases with increasing height.

The CFD code VECTIS has been validated for airflows over both research ships (Yelland *et al.*, 2002) and a surface-mounted block (Moat *et al.*, 2003). Both studies compare the CFD simulations with *in situ* wind speed measurements. Except when the anemometers are located within the wake of an upstream obstacle, or within the decelerated region above the bridge of a tanker/bulk carrier, VECTIS is believed to be accurate to within $\pm 4\%$ in predicting the airflow over ships.

Moat (2003) performed a number of experimental studies and showed that the pattern of the flow above the bridge of a tanker/bulk carrier scaled with the bridge top to deck height. Figure 6 shows the variation of the normalized wind speed with height ($z/H$, where $H$ is the bridge-to-deck height) at a scaled distance of $x/H = 0.5$ back from the upwind edge of the bridge (Moat *et al.*, 2004). The profile was normalized by the free stream or undistorted flow, obtained from a CFD simulation with no model present. The dashed line indicates a normalized wind speed of 1.0, where the wind speed equals the free stream wind speed. The negative normalized wind speed close to the bridge top indicates a flow counter to the mean flow direction. The wind speed maximum increases with distance back from the upwind leading edge (Figure 7) and reaches a maximum of 1.11 at a distance of $x/H = 0.5$. It then reduces to 1.05 at a distance of $x/H = 0.75$.

For container ships the bridge-to-deck height $H$ is denoted as the height of the bridge above the containers. However, the flow above the bridge is also influenced by the large upwind obstacle to the flow presented by

 

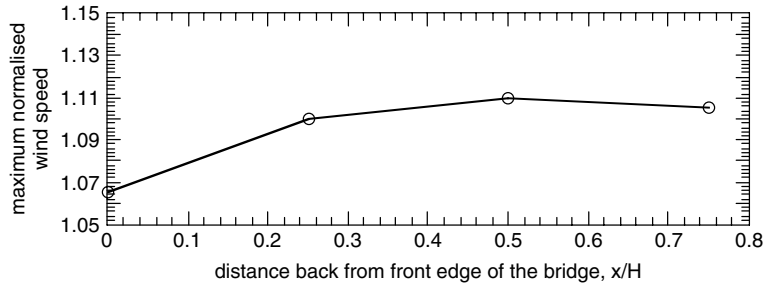


Figure 7. The CFD predicted wind speed maximum at scaled distances back from the front edge of the tanker/bulk carrier bridge ($x/H = 0 = z/H$). The wind speed has been normalized by the free stream, or undisturbed, wind speed profile. Adapted from Moat *et al.* (2004)

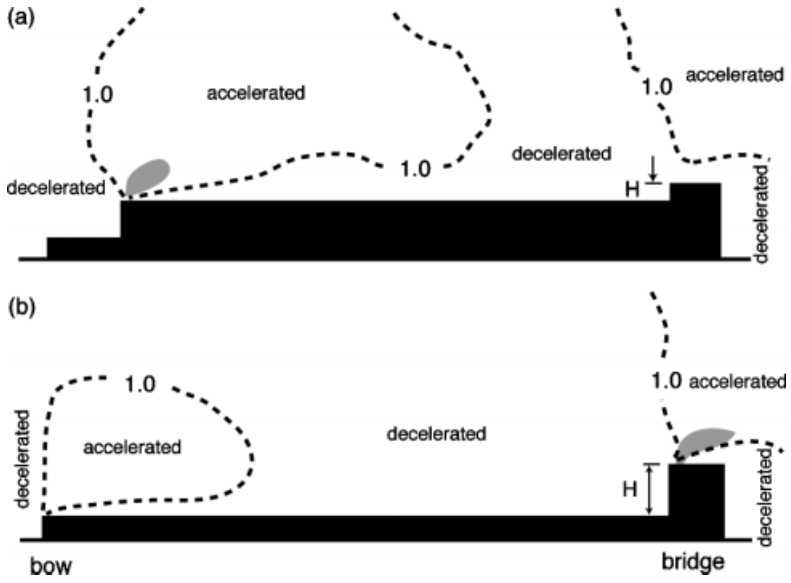


Figure 8. An illustration showing the influence of the size of the bow on the airflow over the bridge of (a) a container ship and (b) a tanker. The dashed lines indicate a normalized wind speed of 1.0, where the wind speed equals the free stream wind speed, and the shaded areas indicate regions of air accelerated by between 8 and 11%. The mean airflow is from left to right and the scaling parameter $H$ for both ships is indicated

the containers themselves (Figure 8). It is currently unclear what effect the irregular loading of the containers will have on the airflow across them and, consequently, on the pattern of the airflow above the bridge. Therefore, Figures 6 and 7 cannot be applied to container ships, and this will be the subject of future work. This research will also examine the effect of the aft loading of containers on the airflow above the bridge.

Some ships carry anemometers on a mast located in the bow rather than above the bridge. The above results for the tanker/bulk carrier may also be applied directly to these cases (using the deck-to-water line height as the scaling parameter $H$) as long as the mast is well upwind of the ship's superstructure or container stacks, which may produce a standing vortex.

## 4. IMPACT OF AIRFLOW DISTORTION ON VOS WIND SPEEDS

### *4.1. Measured wind speed*

It was shown in the previous section that the bias in the measured wind speed reported by a VOS clearly depends on both the ship type and the anemometer position. As part of the VOSClim project (JCOMM,

 

Table III. Estimates of the bridge top to deck height $H$ and the scaled anemometer height $z/H$ for a number of tankers/bulk carriers of various lengths. The anemometer heights above the deck were taken from Kent and Taylor (1991)

| LOA (m) | Anemometer height above deck $z$ (m) | Bridge top to deck height, $H = 9.11 + 0.026 \times \text{LOA}$ | $z/H$ |
|---|---|---|---|
| 293 | 9.3 | 16.73 | 0.56 |
| 293 | 7.0 | 16.73 | 0.42 |
| 108 | 10.0 | 11.92 | 0.84 |
| 231 | 10.0 | 15.12 | 0.66 |
| 290 | 6.4 | 16.65 | 0.38 |
| 290 | 6.4 | 16.65 | 0.38 |
| 206 | 9.1 | 14.47 | 0.63 |
| 290 | 6.4 | 16.65 | 0.38 |
| 290 | 6.4 | 16.65 | 0.38 |

2002), information on ship type and dimensions is being gathered for a subset of VOS, but the required information on anemometer positions is still lacking. Therefore, it is difficult to quantify the influence of the airflow distortion on current VOS measurements as a whole. However, the Voluntary Observing Ships' Special Observing Project–North Atlantic (VSOP–NA) selected a subset of 45 VOS operating in the North Atlantic and produced detailed descriptions of the ship type and instrumentation used (Kent and Taylor, 1991). Of the 16 ships that reported a fixed anemometer above the bridge, the majority were container ships. Only nine ships reported the height of the anemometer above the bridge top, and this varied between 6 and 10 m (Table III). If it can be assumed that these positions are typical for tankers/bulk carriers, as well as for container ships, then it is possible to estimate the biases in wind speed. Using the linear regression (Table I) to predict the tanker/bulk carrier bridge-to-deck height $H$, the anemometer height $z/H$ is seen to vary between 0.4 and 0.8. This suggests that the majority of anemometers are located outside the decelerated region and that wind speed measurements will have a positive bias of between 3 and 11% for anemometers located between the front edge of the bridge ($x/H = 0.0$) and $x/H = 0.75$. A method to predict the wind speed bias for known anemometer locations on tankers/bulk carriers will be the subject of a future paper.

Dobson (1981) stressed the importance of the need to correct for flow distortion and recommended that if height corrections are to be applied to measured wind speeds then flow distortion should also be allowed for. In a comparison of wind speeds from VOS and moored buoys, Thomas *et al*. (2005) showed that correction for height and the effects of atmospheric stability reduce both bias and scatter between pairs of VOS and buoy wind speeds, leaving residual biases of up to 8%. Residual biases vary with VOS type and relative wind direction (Thomas and Swail, 2003) and may, therefore, result from airflow distortion. Particular ship types dominate some merchant ship routes. This could lead to geographic wind speed biases, as the wind speed bias above the bridge may change with VOS type. For example, Thomas *et al*. (2005) showed that there was a change in the wind speed bias between government and non-government ships that lead to differences in the ship reports from the east and west coast of Canada.

### *4.2. Bulk calculations of fluxes*

VOS weather reports are used in the short term for forecast models, etc. In addition, the data are used to produce climatologies of surface fluxes (Josey *et al*., 1999). The mean reported parameters of wind speed and air (AT) and sea-surface temperature (SST) are used to estimate the surface fluxes of heat and momentum in neutral stability conditions via bulk formulae:

$$\text{transfer coefficient} \qquad c = a + bU_{10\text{n}}$$

$$\text{momentum flux} \qquad \tau = \rho c U_{10\text{n}}^2$$

 

sensible heat flux $Q_H = cU_{10n}(AT - SST)$

where $\rho$ is the air density, $U_{10n}$ is the wind speed at a height of 10 m. It can be seen that any bias in the wind speed measurements will lead to a biased flux. For instance, a 10% positive bias in wind speed applied to a $U_{10n}$ of 10 m $s^{-1}$ leads to a 27% overestimate of the momentum flux when calculated via a bulk parameterization (e.g. Smith, 1980). The exchanges of heat between the atmosphere and the ocean are also dependent on the wind. The sensible heat flux $Q_H$ corresponds to a loss or gain of energy by the ocean, depending on the sign of the temperature difference between the ocean surface and the air. The latent heat flux $Q_E$ is the heat exchanged between the sea and the atmosphere by evaporation. In both cases the heat flux is directly proportional to the wind speed (assuming the transfer coefficients for the latent and sensible heat fluxes are constant) and any change due to airflow distortion will be transferred to the bulk calculation of the flux, i.e. a 10% wind speed error will produce a 10% error in the heat flux.

## 5. CONCLUSIONS

Initial results of numerical studies of flow over generic VOS shapes have shown that wind speed measurements made from anemometers located above the bridge may suffer biases of between $-100\%$ and $+11\%$. The numerical studies are believed to be accurate to within $\pm 4\%$ in the region of accelerated flow. The magnitude of the bias depends on ship type and size and the location of the anemometer relative to the superstructure. At present it is not possible to correct VOS observations directly for the effects of flow distortion, since the relevant information on anemometer location is not available. It is hoped that the VOSClim metadata may go some way towards rectifying this issue in the future. Until such information is available, it is only possible to compare observations between different types and sizes of ship in order to estimate biases that may be attributable to flow distortion effects.

The results of the present study can be used in order to site instruments in locations where the effects of flow distortion are minimized. A mast in the bows of the ship, well upwind of any obstruction, is the ideal location, but this is not usually available on VOS. Anemometers located above the bridge of VOS should be placed as far forwards as possible and as high as possible, ideally on a slim mast located at the forward edge of the bridge. If an anemometer cannot be located at the front edge of the bridge then it should be located above a height of the order of $z/H = 0.3$ in order to measure wind speeds outside the decelerated region. An anemometer should not be placed close to the line of equality (normalized wind speed of 1.0), as high velocity gradients are present in this region.

ACKNOWLEDGEMENTS

We wish to thank Dr Peter K. Taylor (Southampton Oceanography Centre, UK) and Val Swail (Meteorological Service of Canada) for their support and encouragement. This project was partially funded by the Meteorological Service of Canada and the Woods Hole Oceanographic Institution.

REFERENCES

Aage C, Hvid S, Hughes PH, Leer-Anderson M. 1997. Wind loads on ships and offshore structures estimated by CFD. In *8th International Conference on the Behavior of Offshore Structures BOSS'97*, Delft.

Blanc TV. 1986. Superstructure flow distortion corrections for wind speed and direction measurements made from Tarwa class (LHA1–LHA5) ships. NL Report 9005, Naval Research Laboratory, Washington, DC.

Blanc TV. 1987. Superstructure flow distortion corrections for wind speed and direction measurements made from Virginia class (CGN38–CGN41) ships. NL Report 9026, Naval Research Laboratory, Washington, DC.

Ching JKS. 1976. Ships influence on wind measurements determined from BOMEX mast and boom data. *Journal of Applied Meteorology* **15**: 102–106.

Diaz H, Folland C, Manabe T, Parker D, Reynolds R, Woodruff S. 2002. Workshop on advances in the use of historical marine climate data. *WMO Bulletin* **51**: 377–380.

Dobson FW. 1981. Review of reference height for and averaging time of surface wind measurements at sea. World Meteorological Organisation, Marine Meteorology and Related Oceanographic Activities Report No. 3. World Meteorological Organization, Geneva.

 

Dupius H, Guerin C, Hauser D, Weill A, Nacass P, Drennan WM, Cloche S, Graber HC. 2003. Impact of flow distortion corrections on turbulent fluxes estimated by the inertial dissipation method during the FETCH experiment on R/V *L'Atalante*. *Journal of Geophysical Research* **108**(C3): 12-1–12-17.
Gill GC, Olsson LE, Sela JS, Suda M. 1967. Accuracy of wind measurements on towers and stacks. *Bulletin of the American Meteorological Society* **48**: 665–674.
ISL. 1997. *Shipping Statistics Yearbook*. Institute of Shipping Economics and Logistics: Bremen, Germany.
JCOMM. 2002. Voluntary Observing Ships (VOS) Climate Subset Project (VOSCLIM) — Project Document — Revision 2. JCOMM Technical Report Series Report No. 5, WMO/TD-No. 1122. World Meteorological Organization, Geneva.
Jin E, Yoon J, Kim Y. 2001. A CFD based parametric study of the smoke behaviour of a typical merchant ship. In *Practical Design of Ships and Other Floating Structures*, Wu Y-S, Cui W-C, Zhou G-J (eds). Elsevier Science.
Josey SA, Kent EC, Taylor PK. 1999. New insights into the ocean heat budget closure problem from analysis of the SOC air–sea flux climatology. *Journal of Climate* **12**(9): 2856–2880.
Kahma KK, Leppäranta M. 1981. On errors in wind speed observations on R/V *Aranda*. *Geophysica* **17**(1–2): 155–165.
Kent EC, Taylor PK. 1991. Ships observing marine climate: a catalogue of the Voluntary Observing Ships participating in the VOSP–NA. World Meteorological Organization, Marine Meteorology and Related Oceanographic Activities Report No. 25.
Kidwell KB, Seguin WR. 1978. Comparison of mast and boom wind speed and direction measurements on US GATE B-Scale ships, NOAA Technical Report, EDS 28. CEDDA, Washington, DC.
Moat BI. 2003. Quantifying the effect of airflow distortion on anemometer wind speed measurements from merchant ships. PhD thesis, University of Southampton, UK.
Moat BI, Yelland MJ, Molland AF. 2004. Possible biases in wind speed measurements from merchant ships. In *5th International Colloquium on Bluff Body Aerodynamics and Applications*, 11–16 July, University of Ottawa, Ottawa, Canada; 537–540.
Mollo-Cristensen E. 1979. Upwind distortion due to probe support in boundary-layer observations. *Journal of Applied Meteorology* **18**: 367–370.
Popinet S, Smith M, Stevens C. 2004. Experimental and numerical study of the turbulence characteristics of airflow around a research vessel. *Journal of Atmospheric and Oceanic Technology* **12**(10): 1575–1589.
RINA Ltd. 1990–93. *Significant Ships*. The Royal Institution of Naval Architects: London, UK.
Romanov YA, Fedorova IB, Chervyakov MS, Shapiro GI. 1983. An improvement in the accuracy of shipboard measurements of wind speed and direction based on aerodynamic tests of a ship model. *Oceanology* **23**(2): 267–270.
Smith SD. 1980. Wind stress and heat flux over the ocean in gale force winds. *Journal of Physical Oceanography* **10**: 709–726.
Surry D, Edey RT, Murley IS. 1989. Speed and direction corrections factors for ship borne anemometers. Engineering Science Research Report BLWT-SS9-89, University of Western Ontario, London, ON, Canada.
Thiebaux ML. 1990. Wind tunnel experiments to determine correction functions for shipborne anemometers. Canadian Contractor Report of Hydrography and Ocean Sciences 36, Bedford Institute of Oceanography, Dartmouth, NS, Canada.
Thomas BR, Swail VR. 2003. Effect of vessel type and platform relative wind direction on comparison between ship and buoy wind speeds. In *Proceedings of CLIMAR-II, 2nd JCOMM Workshop on Advances in Marine Climatology*, Brussels, Belgium, 17–22 November, WMO/TD-No. 1199, JCOMM Technical Report No. 22, CD-ROM.
Thomas BR, Kent EC, Swail VR. 2005. Methods to homogenize wind speeds from ships and buoys. *International Journal of Climatology* **25**: 979–995; this issue.
Yelland MJ, Moat BI, Taylor PK, Pascal RW, Hutchings J, Cornell VC. 1998. Wind stress measurements from the open ocean corrected for airflow distortion by the ship. *Journal of Physical Oceanography* **28**(7): 1511–1526.
Yelland MJ, Moat BI, Pascal RW, Berry BI. 2002. CFD model estimates of the airflow over research ships and the impact on momentum flux measurements. *Journal of Atmospheric and Oceanic Technology* **19**(10): 1477–1499.

 